

Article

Settlement of a Foundation on an Unsaturated Sandy Base Taking Vibrocreep into Account

Armen Z. Ter-Martirosyan * , Alexander N. Shebunyaev  and Evgeny S. Sobolev

Department of Soil Mechanics and Geotechnical Engineering, National Research Moscow State Civil Engineering University, 26, Yaroslavskoye Shosse, 129337 Moscow, Russia; shebunyaev95@mail.ru (A.N.S.); soboleves@mgsu.ru (E.S.S.)

* Correspondence: gic-mgsu@mail.ru

Abstract: Dynamic loading causes (1) a substantial change in the strength and deformation parameters of sandy soil and (2) excessive viscoplastic deformation. The goal of this study is to create a new analytical solution to the problem of the settlement of (1) the foundation that is the source of dynamic loading, and (2) a nearby foundation, taking into account the rheological properties of sandy soil subjected to vibration, given that these rheological properties depend on shear stresses. The proposed solution allows the progress of deformation over time to be described. The present paper states and provides an analytical solution for the problem of evaluating the settlement of a single foundation that transmits static and dynamic harmonic pressure to the base. The authors also analyze the settlement of another foundation located at some distance from the transmitting foundation. The second foundation transmits static pressure to the base. The dependence of the viscosity coefficient on the shear stress intensity and vibration intensity, as well as the vibrocreep decay over time, are based on the exponential and homographic dependencies previously identified by two of the authors (A.Z. Ter-Martirosyan and E.S. Sobolev). The solution to the problem is obtained by numerical integration in the Mathcad program of an analytical expression for nonlinear viscoplastic deformations. As a result of the research, the authors have found that the dynamic viscoplastic component makes the greatest contribution to foundation settlement. The settlement of the transmitting foundation increases along with increasing static and dynamic pressure transmitted to the base. The settlement of the nearby foundation increases when the pressure increases under the foundation, but it reduces when static pressure from the transmitting foundation, the depth of the foundation, and the distance between the foundations increase. General analytical dependencies obtained by the authors comply with the results of laboratory and field experiments performed by other researchers. These dependencies can be used to predict the settlement of foundations in whose unsaturated sandy bases mechanical vibrations propagate.

Keywords: excessive foundation settlement; foundation vibrations; dynamic cyclic loading; vibrocreep of sandy soil; viscosity of sandy soil; numerical integration in Mathcad; mathematical analysis of nonlinear soil deformation

MSC: 74L10



Citation: Ter-Martirosyan, A.Z.; Shebunyaev, A.N.; Sobolev, E.S. Settlement of a Foundation on an Unsaturated Sandy Base Taking Vibrocreep into Account. *Axioms* **2023**, *12*, 594. <https://doi.org/10.3390/axioms12060594>

Academic Editor: Nhon Nguyen-Thanh

Received: 17 May 2023
Revised: 12 June 2023
Accepted: 14 June 2023
Published: 15 June 2023



Copyright: © 2023 by the authors. Licensee MDPI, Basel, Switzerland. This article is an open access article distributed under the terms and conditions of the Creative Commons Attribution (CC BY) license (<https://creativecommons.org/licenses/by/4.0/>).

1. Introduction

The safety of industrial and civil buildings and structures must be evaluated throughout their lifecycles if these buildings and structures are subjected to dynamic effects from various sources [1,2]. Such sources encompass various fixed and mobile machines and mechanisms, traveling road and rail vehicles, earthquakes, etc. In practice, dynamic loading may have a wide range of adverse effects on the performance of bases and foundations, ranging from slow long-term accumulation of settlements to higher-than-normal continuous settlements, causing critical damage to foundations and superstructures.

For example, according to R.A. Ershov and A.A. Romanov, the average annual settlement of buildings located within 30 m from the axis of highways is 0.3–2.2 mm/year [3]. Any excessive settlements, caused by the cyclic loading of the sand base, can also worsen the operating parameters of the equipment installed inside due to warping and eccentricities [4]. Cases of excessive settlement, reaching 28 cm, were registered in the plant building area where a swaging machine was in operation. As for another plant building, the settlements of column foundations reached 40 cm in the area where a drop forging hammer was in operation [3]. According to the observations of D.D. Barkan [5,6], a drop forging hammer weighing 4.5 tons that was in operation in a production shop caused excessive settlement of an adjacent brick building located within the plant territory. Eventually, its settlement led to its failure. In his work, V.M. Pyatetsky [7] provides an extensive list of 25 facilities where critical structural damage was observed (cracks in bearing walls, excessive deformations of the framework, deformations of crane tracks, disintegrated column–truss joints, etc.). Settlements were observed at a distance of up to 20–30 m from the source of dynamic loading (compressors, sawmills, crushing machines, ore grinders, etc.). According to other researchers, the maximum value of settlement reaches 88 cm [3,8–10].

Changes in the deformation and strength properties of sandy soils subjected to dynamic loads are important factors in predicting the stress–strain state of the bases of building structures [1,2,11]. Engineering practice is aware of a large number of structural failures caused by the vibrocreep of sandy soils. These failures were manifested as the substantial settlement of bases (including those described above), damaged building structures, and the collapse of entire buildings, which most clearly demonstrate the relevance of this issue. A study on the phenomenon of vibrocreep of sandy soils was initiated in the first half of the 20th century and it gained increasing interest in 1960–1980 due to the widespread implementation of industrial construction projects accompanied by the installation of powerful sources of dynamic loading [12]. Most of the works in this subject area focus on the study of the deformation and stability of saturated sandy bases since pore pressure increases under dynamic loading and vibration-induced liquefaction of the foundation occurs, which can lead to the rapid destruction of structures. However, many authors study the deformation of unsaturated sandy soils.

An important contribution to the study of vibrocreep processes was made by the outstanding scientist D.D. Barkan [1,2], who conducted initial experiments focused on the identification of the viscosity coefficient. In the course of his experiments, a ball was immersed in sandy soil under vibration. D.D. Barkan conducted a simple laboratory experiment to demonstrate that sandy soil develops rheological properties if subjected to vibration, and the viscosity coefficient of sandy soil depends on vibration acceleration. Of particular interest, is the work of V.A. Ilyichev, V.I. Kerchman, B.I. Rubin, and V.M. Pyatetsky, in which the authors described a large-scale field experiment consisting of the field observation of vibrations and settlement of seven experimental foundations of different sizes and pressure under the foundation. In this experiment, one of the foundations was the source of the vibrations [7,10,13]. The authors discovered the effect of static and dynamic pressure under the foundation on the manifestation of vibrocreep. V.S. Bogolyubchik, M.N. Goldstein, and V.Ya. Khain conducted numerous flume and field tests to simulate foundation displacement under dynamic loading [14–16]. Results obtained by D.F. Gil et al. from flume testing [17] demonstrate a decrease in the stability of the sandy base under cyclic loading when there is an increase in the frequency and amplitude of vertical vibrations. Flume tests, involving the cyclic loading of a sandy base model, were conducted by K. Al-kaream et al. [18] and showed the accumulation of plastic deformations over time with the final stabilization of the deformation process. The work of J. Wang et al. [19] reports the results of large-scale laboratory studies on the mutual effect of two closely located foundations on a sandy base subjected to cyclic loading based on the depth and distance between them. The authors show that if the two foundations are subjected to cyclic loading, the greatest bearing capacity is observed if the distance between the foundations is equal to twice the width of the foundation base. The works

report the regularity of settlement development over time at different values of soil density, static loading, and foundation depth. The conclusions drawn by the above researchers are important practical materials for evaluating the results of the theoretical solution to the problem described in this work.

Early studies on the behavior of soils under dynamic loading were conducted by A. Casagrande and W.L. Shannon during the construction of the Panama Canal [20]. The tremendous loss of life and destruction of civil infrastructure facilities built on saturated sand bases and the collapses of hydraulic facilities as a result of the earthquakes in the US and Japan in 1960–1970, coupled with the launched construction of nuclear power plants, served as the reason for the intensive research of the behavior of sandy soils under dynamic loading. The publication written by H.B. Seed and K.L. Lee [21] reaches an important conclusion about the effect of lateral compressive pressure σ_3 on the number of loading cycles that cause soil failure. Studies by K.L. Lee and J. Focht [22] showed that, for practical purposes, the relationship between dynamic strength and effective pressure σ_3 can be taken as a direct dependence for a small range of stresses. Researchers R.C. Chaney and H.Y. Fang [23] studied the behavior of dry sandy soils subjected to cyclic loading and showed that axial deformation accumulates in the course of small-amplitude dynamic loading, and, following a number of cycles, the hysteresis loop closes and the specimen stabilizes. According to V.K. Khosla and R.D. Singh [24], if the dynamic stress amplitude σ_d increases or the lateral compressive pressure σ_3 decreases, the stable state of the soil is replaced by the slow accumulation of deformations (vibrocreep).

A wide range of modern studies on the vibrocreep of sandy soils was conducted by two of the current study's authors (AZT-M and ESS) and Z.G. Ter-Martirosyan. The authors believe that under compression an increase in plastic deformations decays alongside an increase in the number of cycles and that in the case of low-frequency cyclic loading (up to 1–2 Hz), frequency has no significant effect on deformation propagation (the difference does not exceed 2% for the same number of loading cycles), while the number of loading cycles and soil density have a strong effect when the number and amplitude of the cyclic loading are at a maximum [25,26]. Vibrocreep coefficients for compression and shear differ significantly (up to 10 times). Hence, soils are more sensitive to shear vibration than to compression vibration [25,27]. In cases of cyclic and vibratory loading, additional deformations increase with increasing static shear stresses and decrease with increasing mean stresses. Therefore, these deformations depend on the proximity to the limiting state [25,27,28]. In the case of a vibratory action, vibrocreep-induced deformation increases with increasing frequency and decays in time [25,27]. Viscosity increases during loading, and by the time the vertical deformations stabilize, viscosity values approach the values obtained during the tests conducted at low velocities (nearly static ones). Viscosity plummets at the onset of loading, which causes vertical deformations to spike. Then, as the testing progresses, soil density increases, viscosity gradually increases, and vertical deformations stabilize. At the onset of a dynamic test, the viscosity differs from the "static" viscosity by a factor of 100. Hence, during dynamic loading, soil behaves as a non-Newtonian fluid [25,27,29]. E.A. Voznesensky conducted a wide range of research on the behavior of sandy bases and evaluated the development of deformations over time and the effect of the amplitude of dynamic pressure [12].

Liu X. et al. [30] compare the deformation of sand specimens subjected to static and cyclic loading and demonstrate the effect of cyclic loading and relative density on cyclic strength. M. Poblete et al. [31] describe a succession of sand tests whereby sand was subjected to various values of compressive pressure and vibration amplitudes under cyclic loading. B. Kafle and F. Wuttke [32] have found that in the case of cyclic loading, dry sand accumulates deformations more intensively than wet unsaturated sand. Each cycle makes the accrual of plastic strain smaller, but even with a large number of cycles, the strain does not reach any final value.

K. Wang et al. [33] studied the effect of lateral compressive pressure on the intensity of axial and volumetric deformation of sandy soil subjected to cyclic loading. It was

recorded that at a certain value of lateral compressive pressure the specimen did not collapse due to significant expansion (dilatancy), as it was recorded at lower values of σ_3 , but its compaction occurred due to the increasing axial deformation and destruction of soil particles, which was also mentioned in the work of one of the current authors (AZT-M) [25]. This paper also describes the breakdown of deformation mechanisms of sandy soil subjected to cyclic load into plastic compaction, vibrocreep, and continuous plastic failure. The authors describe the deformation of sandy soil using an analytical dependence in which values of vertical σ_1 and lateral σ_3 stresses are used. Similar results are reported in the studies of Y. Jianhong et al. [34], where the authors use the case of triaxial tests to demonstrate three stages of soil deformation before failure: the elastoplastic stage, the slow creep stage, and the fast creep stage at different values of compressive pressure and vertical loading. The work by Dong-Ning D. et al. [35] has an analytical description of the rheological model describing this staged viscoplastic behavior of sandy soils subjected to vibration. The results of research performed by Y. Liu et al. [36] show a significant increase in transverse deformation in the case of cyclic loading; this feature is observed up to a certain value of axial deformation (in the authors' work it is 6%), and if it is exceeded, cyclic loading has no effect on transverse deformation even at different values of relative density and amplitude of cyclic deformation. The article written by D.F. Gil et al. [17] reports the effect of the frequency of dynamic loading on soil deformation.

Z. Wang and L. Zhang [37] show the effect of cyclic deformation amplitude, lateral compressive loading, the ratio of vertical and lateral static stresses, and vibration frequency on axial deformation and stiffness of sandy soil subjected to cyclic loading. A. Kumar et al. [38] present the results of triaxial tests of embankment soil of a railroad track at different vibration frequencies and show that an increase in frequency reduces soil stiffness to some extent, but any further increase in frequency does not lead to a substantial reduction in stiffness. The results of D. Song et al. [39] and W. Ma et al. [40] show how the shear modulus changes under cyclic loading at different angular deformation and compressive pressure values. It is found that the deformation modulus decreases significantly with increasing angular deformation during vibration, but this decrease reduces significantly with increasing compressive pressure. In addition, W. Ma et al. [40] investigated the effect of the intensity of static and dynamic components of loading on a decrease in its shear modulus. The authors provide an analytical relationship to take into account a decrease in the shear modulus using experimental parameters and the value of angular deformation. P. Xia et al. [41] propose an analytical dependence describing the vibration of soil under dynamic loading and breakdown into elastic and plastic components. Dependencies identified by the authors in respect of strain and shear moduli are also applicable to this study in terms of a reduction in the viscosity coefficient if the soil deformation over time and damping creep are considered.

The numerous works mentioned above offer a nearly exhaustive description of the deformation of sandy soil over time under cyclic loading taking into account the effect of the frequency and amplitude of dynamic impacts, the static loading, and the lateral pressure. This study, describing the process of deformation of sandy soil under dynamic loading, employs a rheological model that takes into account dependencies obtained earlier by the researchers of NRU MGSU of the effect of vibration acceleration, the proximity to the limit state, and the nature of deformation over time [25–28]. These dependencies are consistent with the results obtained by other researchers.

Publicly available articles offer numerical solutions to the problem of settling foundations resting on sandy non-saturated bases and subjected to dynamic loading (e.g., works written by Vivek P. and Ghosh P. [42], Wichtmann T. et al. [43], Wuttke F., Schmidt H.G., Zabel V. et al. [44]) or analytical solutions obtained by introducing reduced deformation characteristics of soils into soil analysis (e.g., Yi F. [45,46] and Pradel D. [47] suggest calculating settlement using angular deformation by taking into account a reduction in the shear modulus and soil porosity; one of the current authors (ESS) [48] suggests reducing the deformation modulus of the base by taking into account the vibrocreep coefficient).

At the same time, there are no analytical solutions obtained using the rheological model of sandy soil that allow for the accurate identification of dependencies and mathematical analysis of the effect of each factor separately. To fill this gap, the authors propose a new analytical solution to the problem of settlement of a single foundation subjected to dynamic harmonic loading and an adjacent foundation subjected to static loading.

Hence, the researchers identified several dependencies determining the deformation of sandy non-saturated soil for various parameters of dynamic loading. However, a review of solutions to problems of foundation settlement shows that authors do not use any currently available rheological models to describe deformation in their computational models. Moreover, the heterogeneous stress–strain state is formed in a foundation with varying proximity of tangential stress intensity to its limit value, which should also be taken into account in projections of foundation settlements. The purpose of this study is to propose a new solution to the analytical problem of foundation settlement under dynamic loading taking into account the vibrocreep of sandy soil with a changing viscosity coefficient, which depends on the stress level, vibration intensity, and time.

2. Materials and Methods

We consider the propagation of the settlement of a single foundation that has width $b_1 = 2 \cdot a_1$, and is located at depth h_1 (see Figure 1). The foundation is subjected to static load N_1 and dynamic harmonic load $\Delta N \cdot \sin(\omega \cdot t)$, which trigger pressures p_1 and $\Delta p \cdot \sin(\omega \cdot t)$ below the foundation base, resting on the homogeneous unsaturated sandy base, characterized by gravity γ , internal friction angle φ , deformation modulus E , Poisson’s ratio ν and viscosity coefficient η_0 during manifestations of vibrocreep, the rheological parameter of strengthening at vibration creep α and coefficient δ , showing the dependence of viscosity on vibration acceleration using the case of a refractory tube mill (width of foundation $b_1 = 7.2$ m, static pressure below the foundation base $p_1 = 160$ kPa, the amplitude of dynamic pressure $\Delta p = 30$ kPa, frequency of loading $\omega = 10$ Hz).

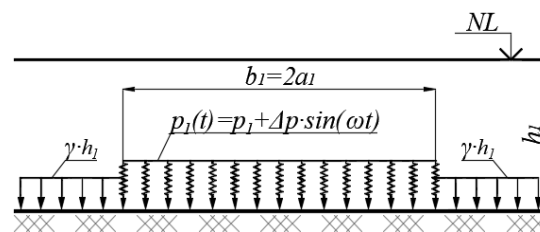


Figure 1. Loading diagram.

The base has a layer of unsaturated fine sand having the following principal design characteristics: $\gamma = 19.6$ kN/m³; $\varphi = 30.3^\circ$; $E = 30.2$ MPa; $\nu = 0.3$; $\alpha = 0.015$; $\Delta = 9.9$; $\eta_0 = 2.76 \cdot 10^5$ Pa·s. Information about the particle size distribution is provided in Figure 2.

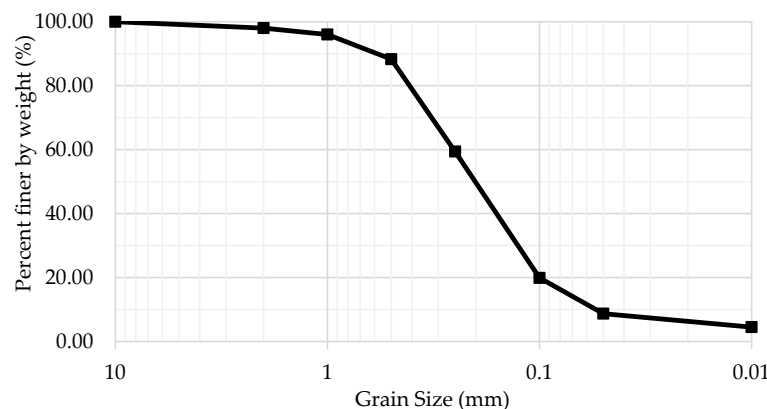


Figure 2. Particle size distribution in a specimen of sand.

A solution is provided for the case of the quasi-dynamic problem statement (with inertial terms being neglected in equations of motion) [49]: the sand medium becomes viscous due to the vibration triggered by the dynamic component of loading [3,6,8,50], and the foundation sinks into the viscous base due to the static component of vertical loading [51]. The foundation settlement in time $s(t)$ is composed of an elastic component s_{st} , which the foundation gets from the static component of loading p_1 before the commencement of operation, and a viscoplastic component $s_{dyn}(t)$, which the foundation gets after the commencement of equipment operation that has a dynamic effect on the base $\Delta p \cdot \sin(\omega \cdot t)$ (1) [3].

$$s(t) = s_{st} + s_{dyn}(t) \tag{1}$$

Elastic settlement s_{st} is calculated according to the well-known dependence (2) [52].

$$s_{st} = \sum_{i=1}^n 0.8 \cdot \frac{\sigma_{zp,i} \cdot h_i}{E_i} \tag{2}$$

where n is the number of layers within the compressible thickness;

$\sigma_{zp,i}$ is an additional stress in the i -th soil layer according to Formula (5);

h_i is the thickness of the i -th soil layer;

E_i is the static deformation modulus of the i -th soil layer.

The viscoplastic component of settlement $s_{dyn}(t)$ is calculated by Formula (3) by integrating the vertical deformations ε_z over the depth of the sand layer [53] using the dependences obtained by authors AZT-M [25,28] and ESS [27] in respect of the propagation of vibrocreep in time, the effect of increasing shear stresses that approach their limit value, and the effect of vibratory acceleration on the viscosity coefficient.

$$s_{dyn}(t) = \int \varepsilon_z^{dyn} dz = \int_0^H \left[\frac{\tau_i}{\alpha \cdot \eta_0 \cdot e^{-\Delta \cdot a} \cdot \frac{\tau_i^* - \tau_i}{\tau_i^*}} \cdot (1 - e^{-\alpha \cdot t}) \right] dz \tag{3}$$

where τ_i is the intensity of shear stresses according to Formula (4);

τ_i^* is the ultimate tangential stress according to Formula (4);

α is the experimental rheological hardening parameter [25,27];

Δ is an experimental coefficient, showing the dependence of viscosity on vibratory acceleration of vibrations [25,27];

a is the vibratory acceleration of vibrations;

η_0 is the viscosity coefficient before the commencement of vibratory loading;

H is the distance from the foundation to the bottom of the sand layer.

$$\begin{aligned} \tau_i^* &= \sigma_m \cdot \text{tg} \varphi \\ \sigma_m &= \frac{\sigma_x + \sigma_y + \sigma_z}{3} \\ \tau_i &= \frac{\sqrt{(\sigma_x - \sigma_y)^2 + (\sigma_y - \sigma_z)^2 + (\sigma_z - \sigma_x)^2 + 6 \cdot (\tau_{xy}^2 + \tau_{yz}^2 + \tau_{zx}^2)}}{\sqrt{6}} \end{aligned} \tag{4}$$

In the case of the application of a uniformly distributed load, expressions for stresses are obtained by G.V. Kolosov (5) [52,54] by integrating the solution of the Boussinesque problem in the case of two dimensions in width $2a$ for a plane strain problem [53,55].

$$\begin{aligned} \sigma_x &= \frac{p}{\pi} \cdot \left(\text{arctg} \frac{a-x}{z} + \text{arctg} \frac{a+x}{z} \right) - \frac{2ap}{\pi} \cdot \frac{z \cdot (x^2 - z^2 - a^2)}{(x^2 + z^2 - a^2)^2 + 4a^2z^2} \\ \sigma_z &= \frac{p}{\pi} \cdot \left(\text{arctg} \frac{a-x}{z} + \text{arctg} \frac{a+x}{z} \right) + \frac{2ap}{\pi} \cdot \frac{z \cdot (x^2 - z^2 - a^2)}{(x^2 + z^2 - a^2)^2 + 4a^2z^2} \\ \sigma_y &= \nu \cdot (\sigma_x + \sigma_z) = \frac{2\nu p}{\pi} \cdot \left(\text{arctg} \frac{a-x}{z} + \text{arctg} \frac{a+x}{z} \right) \\ \tau_{xz} &= \frac{4ap}{\pi} \cdot \frac{x \cdot z^2}{(x^2 + z^2 - a^2)^2 + 4a^2z^2} \end{aligned} \tag{5}$$

By substituting expressions for stress components (5) into expressions (4) at $a_1 = 3.6$ m and $p_1 = 160$ kPa in Mathcad software, we obtain graphs for mean stresses σ_m and shear stress intensity τ_i , shown in Figures 3 and 4, respectively.

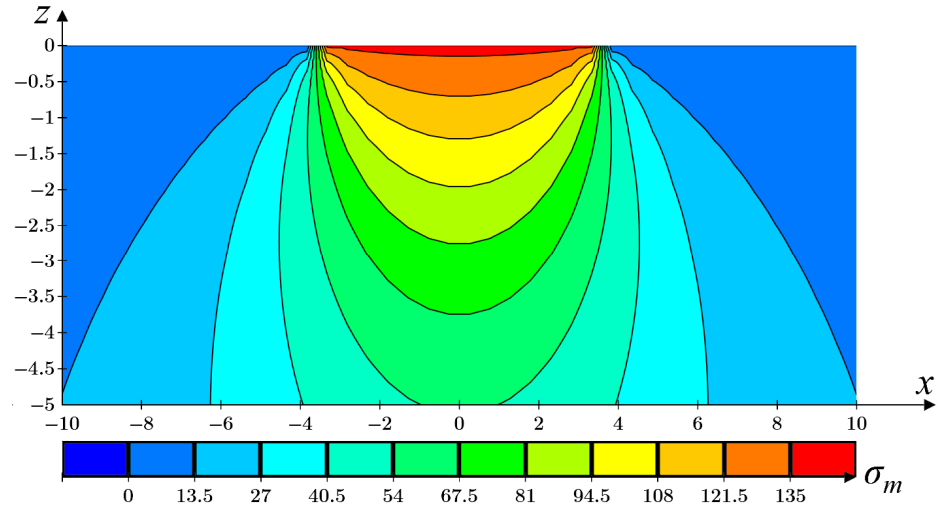


Figure 3. Isofields of mean stresses σ_m in the sandy base at $a_1 = 3.6$ m and $p_1 = 160$ kPa.

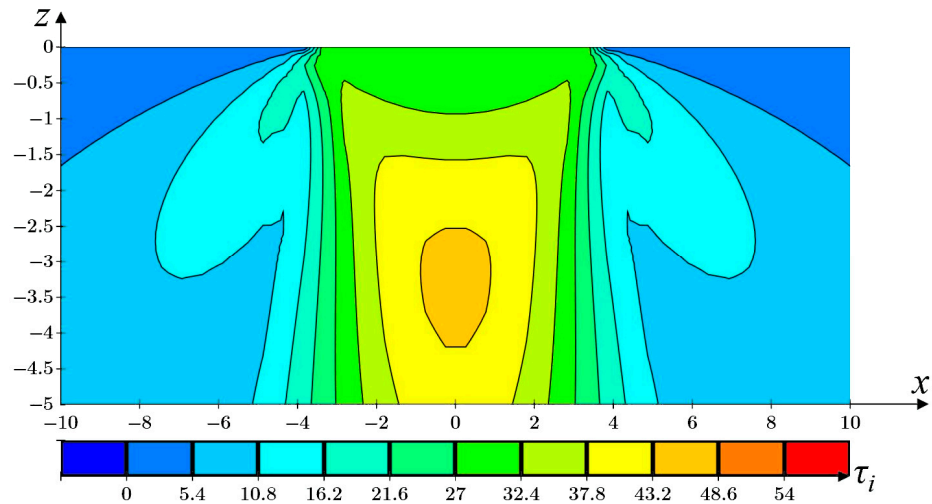


Figure 4. Isofields of the intensity of shear stresses τ_i in the sandy base at $a_1 = 3.6$ m and $p_1 = 160$ kPa.

The value of the vibration amplitude $A_{z,0}$ is found using the well-known Formula (6) [3].

$$A_{z,0} = \frac{\Delta N}{K_Z} \cdot \frac{1}{\sqrt{\left(1 - \frac{\omega^2}{\lambda_z^2}\right)^2 + (\Phi_z \cdot \omega)^2}} \tag{6}$$

where K_Z is the stiffness coefficient of the base;
 λ_z is the frequency of natural vibrations;
 Φ_z is the modulus of decay.

The base stiffness coefficient K_Z is calculated by Formula (7) [3,9,10,52]. The expression for the coefficient C_z in Formula (7) was adopted based on the results of a study by S.K. Lapin, who conducted field experiments on more than 300 foundations with an area of 0.5 to 3700 m² [3]. These results have satisfactory convergence with field experiments and are accepted in the Soviet standard of building design.

$$K_Z = C_z \cdot F = b \cdot E \cdot \left(1 + \sqrt{F_0/F}\right) \cdot F \tag{7}$$

where b is the coefficient, taken as being equal to 1.0 for sands;

E is the soil modulus of elasticity;

$F_0 = 10 \text{ m}^2$;

F is the area of the foundation bottom.

The frequency of the natural vibrations λ_z is calculated by Formula (8) [3,7,10].

$$\lambda_z = \sqrt{\frac{K_z}{M}} \tag{8}$$

The approximate value of the modulus of decay Φ_z can be taken from reference tabular data depending on the type of soil [13] or found by Formula (9) [3].

$$\Phi_z = \frac{2\xi_z}{\lambda_z} = \frac{4\sqrt{M}}{\sqrt{p_m \cdot K_z}} \tag{9}$$

where M is the mass of the oscillating object;

p_m is the average pressure under the foundation.

The amplitude of the vertical vibrations of the soil $A_z(r)$ at distance r from the center of the base of the source of vibrations is determined by Formula (10) [7,9,10,52].

$$A_z(r) = A_{z,0} \cdot \left\{ \frac{1}{\Delta \cdot [1 + (\Delta - 1)^2]} + \frac{\Delta^2 - 1}{\sqrt{3\Delta}(\Delta^2 + 1)} \right\} \tag{10}$$

where $A_{z,0}$ is the amplitude of vertical vibrations of the foundation that is the source of vibrations;

$\Delta = r/r_0$ is the parameter that is equal to the ratio of distance r from the center of the base of the foundation that is the source of vibrations to the reduced radius of that base.

The distribution of vibrations in depth z follows dependence (11) [3,7,52]. It is noteworthy that the amplitude of harmonic vibrations with constant frequency is directly proportional to the acceleration of vibrations, as in a second derivative of displacement, so the following dependence (11) is also true for the distribution of vibration amplitudes with depth.

$$w = w_0 \cdot e^{-\beta z} \tag{11}$$

where w is the acceleration of vibrations in depth z ;

w_0 is the acceleration of the base vibrations at the level of the foundation bottom;

β is the coefficient of decay, whose value is 0.07–0.10 m^{-1} for sandy soils.

The expression for the vibration amplitudes of the base A_z in Mathcad is shown in Figure 5. Vibration amplitude isofields for the sandy base A_z obtained in Mathcad, are shown in Figure 6 for the case where the dynamic load component $\Delta p = 40 \text{ kPa}$ and $\omega = 10 \text{ Hz}$.

$$A_z(x, z, \Delta p, p_1) := \begin{cases} \text{if } |x| \leq r_0 \\ A_{z0}(\Delta p, p_1) \cdot e^{\beta \cdot z} \\ \text{else} \\ A_{z0}(\Delta p, p_1) \cdot \left(\frac{1}{\left| \frac{x}{r_0} \right| \cdot \left(1 + \left(\left| \frac{x}{r_0} \right| - 1 \right)^2 \right)} + \frac{\left(\frac{x}{r_0} \right)^2 - 1}{\sqrt{3 \cdot \left| \frac{x}{r_0} \right| \cdot \left(\left(\frac{x}{r_0} \right)^2 + 1 \right)}} \right) \cdot e^{\beta \cdot z} \end{cases}$$

Figure 5. Expression for vibration amplitudes of the base A_z in Mathcad.

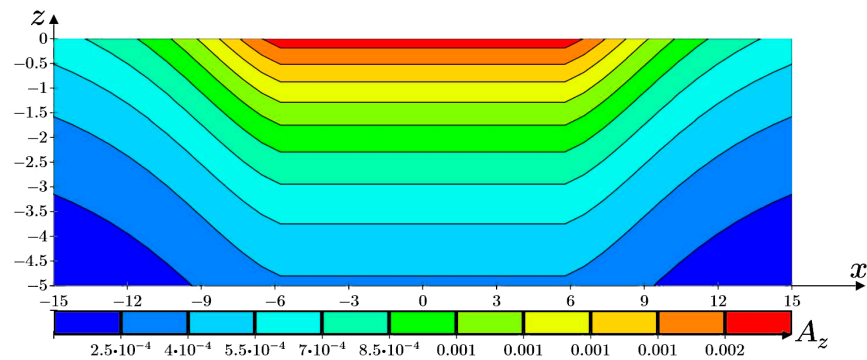


Figure 6. Isofields of vibration amplitudes of the base A_z at $\Delta p = 40$ kPa and $\omega = 10$ Hz.

The expression for the viscoplastic component of settlement s_{dyn} in Mathcad is shown in Figure 7. The expression is obtained by substituting expressions (7–9) in (6), and then (6), (10), and (11) in (3) [56,57].

$$s_{dyn}(x, z, \Delta p, p_1) := \int_0^{-3} \tau_{ii}(x, z, p_1) dz$$

$$= \int_0^{-3} \left[\begin{array}{l} \text{if } |x| \leq r_0 \text{ then } -\delta \cdot \omega^2 \cdot A_{av}(\Delta p, p_1) \cdot e^{\beta \cdot z} \\ \text{else} \\ A_{av}(\Delta p, p_1) \cdot \left(\frac{1}{\left(\frac{|x|}{r_0} \right) \cdot \left(1 + \left(\frac{|x|}{r_0} - 1 \right)^2 \right)} + \frac{\left(\frac{|x|}{r_0} \right)^2 - 1}{\sqrt{3} \cdot \left(\frac{|x|}{r_0} \right) \cdot \left(\left(\frac{|x|}{r_0} \right)^2 + 1 \right)} \right) \cdot e^{\beta \cdot z} \end{array} \right] \cdot \left[\begin{array}{l} \text{if } \frac{\sigma_{m1}(x, z, p_1) \cdot \tan(\varphi) - \tau_{ii}(x, z, p_1)}{\sigma_{m1}(x, z, p_1) \cdot \tan(\varphi)} \leq 0.1 \\ \text{then } 0.1 \\ \text{else} \\ \frac{\sigma_{m1}(x, z, p_1) \cdot \tan(\varphi) - \tau_{ii}(x, z, p_1)}{\sigma_{m1}(x, z, p_1) \cdot \tan(\varphi)} \end{array} \right] \cdot \left[\begin{array}{l} \alpha \cdot \eta_0 \cdot e \\ \text{if } |x| \leq r_0 \text{ then } -\delta \cdot \omega^2 \cdot A_{av}(\Delta p, p_1) \cdot e^{\beta \cdot z} \\ \text{else} \\ A_{av}(\Delta p, p_1) \cdot \left(\frac{1}{\left(\frac{|x|}{r_0} \right) \cdot \left(1 + \left(\frac{|x|}{r_0} - 1 \right)^2 \right)} + \frac{\left(\frac{|x|}{r_0} \right)^2 - 1}{\sqrt{3} \cdot \left(\frac{|x|}{r_0} \right) \cdot \left(\left(\frac{|x|}{r_0} \right)^2 + 1 \right)} \right) \cdot e^{\beta \cdot z} \end{array} \right] \cdot (1 - e)$$

Figure 7. Expression for the viscoplastic component of settlement s_{dyn} in Mathcad.

The above problem of settlement of a single foundation helps to solve another problem of excessive settlement of the foundation of a nearby building. Towards this end, we use the case of an existing finished product screening shop near which a tube mill will be erected. Figure 8 shows photographs of the site that will accommodate the tube mill.

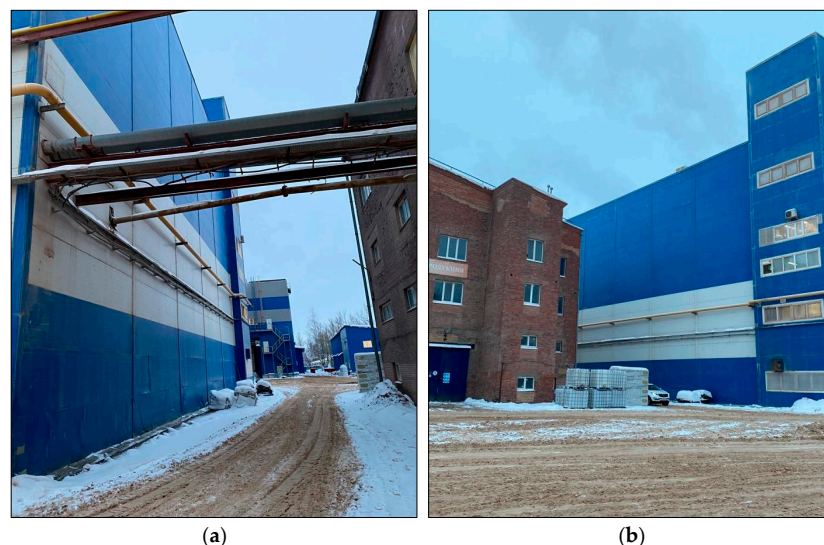


Figure 8. (a,b) The tube mill site between existing workshops.

The foundation plan is shown in Figure 9 and the loading diagram is shown in Figure 10.

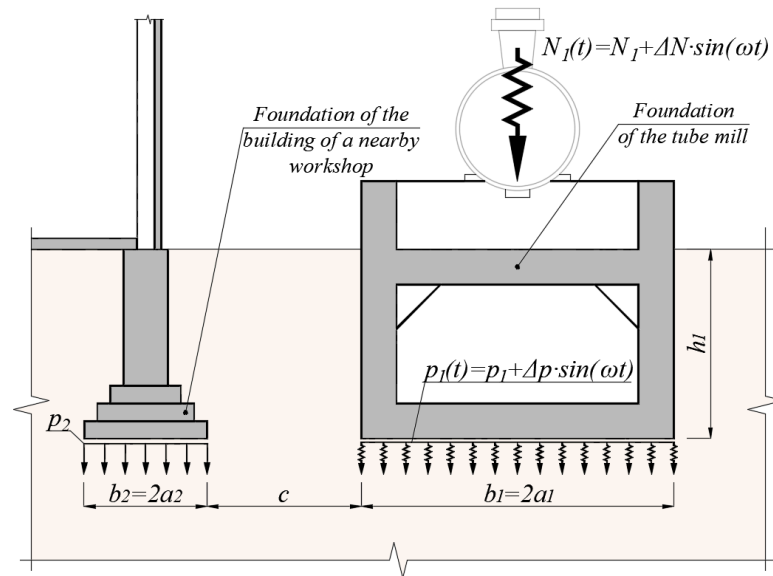


Figure 9. The foundation base plan of the tube mill, which is the source of dynamic loading, and the foundation plan of the building of a nearby workshop.

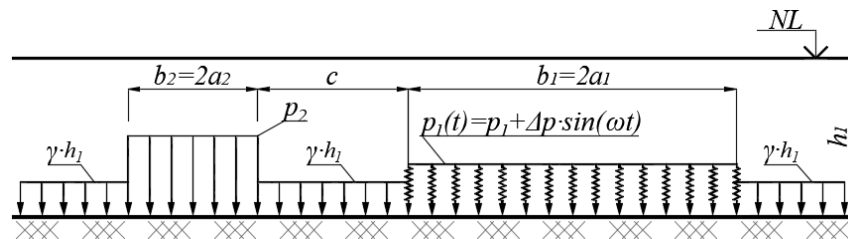


Figure 10. Loading diagram.

By placing the source of loading close to the existing foundations, we trigger additional stresses identified using the expressions obtained by G. Kolosov (5) [52,54].

Figures 11 and 12 show the isofields of mean stresses σ_m and the intensity of shear stresses τ_i in the base subjected to the combined action of loads from the constructed foundation $p_1 = 160$ kPa and the existing foundation $p_2 = 350$ kPa if the half-widths of foundations are $a_1 = 3.6$ m, $a_2 = 1.2$ m, the distance between foundations $c = 4.0$ m, and their depth is $h_1 = 3.8$ m.

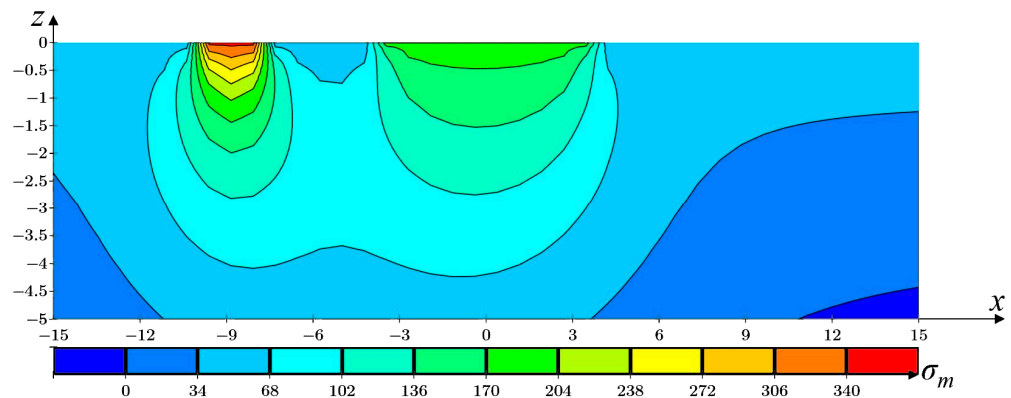


Figure 11. Isofields of mean stresses σ_m in a sandy base.

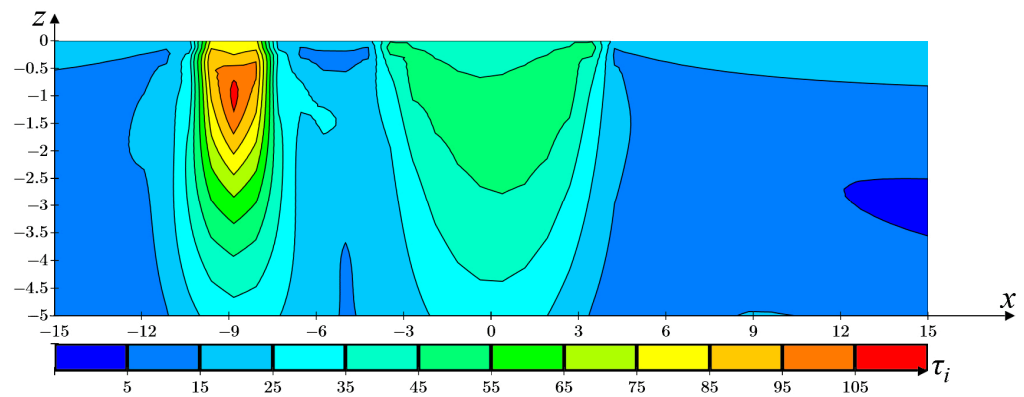


Figure 12. Isofields of stress intensity τ_i in a sandy base.

3. Results

As for a single foundation (Figure 1), if we sum the elastic s_{st} and viscoplastic $s_{dyn}(t)$ components of the settlement calculated using Formulas (2) and (3), we will have a family of foundation settlement curves, as shown in Figure 13.

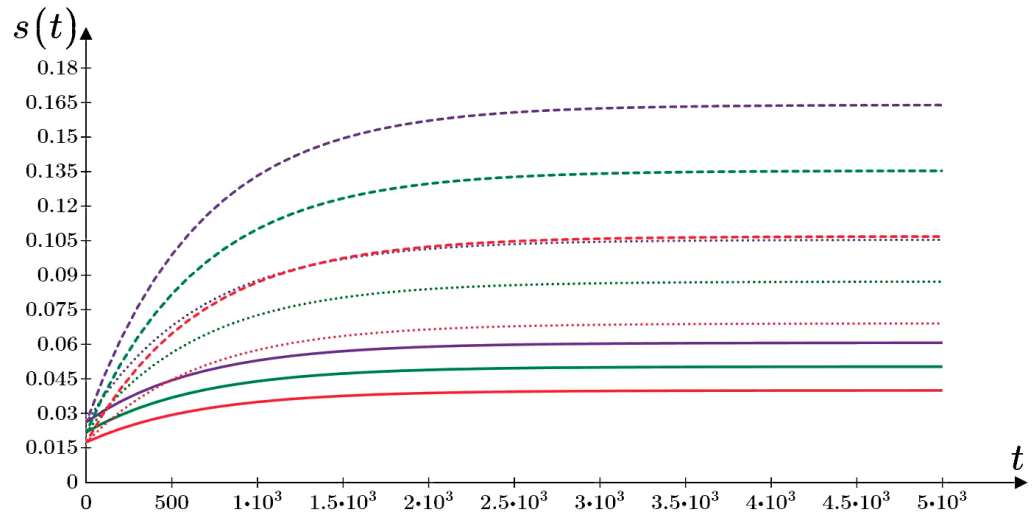


Figure 13. The propagation of foundation settlement in time at static loading p_1 and dynamic loading Δp : (—) $p_1 = 160$ kPa, $\Delta p = 10$ kPa; (·····) $p_1 = 160$ kPa, $\Delta p = 20$ kPa; (- - - -) $p_1 = 160$ kPa, $\Delta p = 30$ kPa; (—) $p_1 = 200$ kPa, $\Delta p = 10$ kPa; (·····) $p_1 = 200$ kPa, $\Delta p = 20$ kPa; (- - - -) $p_1 = 200$ kPa, $\Delta p = 30$ kPa; (—) $p_1 = 240$ kPa, $\Delta p = 10$ kPa; (·····) $p_1 = 240$ kPa, $\Delta p = 20$ kPa; (- - - -) $p_1 = 240$ kPa, $\Delta p = 30$ kPa.

Analysis of Figure 13 makes it clear that, as the static load component p_1 and dynamic load component Δp increase, the foundation settlement increases. Hence, according to the results of Kerchman’s field studies [58], an increase in the dynamic component Δp makes a more substantial contribution by triggering viscoplastic shear of the double-sided extrusion type. This is evident in the nonlinear dependence $s(\Delta p)$ presented in Figure 14. The increase in settlement that accompanies an increase in dynamic component Δp is caused by a decrease in the viscosity coefficient and an increase in vibratory acceleration of the base vibration, while the increase in settlement that accompanies an increase in static component p_1 is triggered by an increase in the intensity of shear stresses in base τ_i and their approaching ultimate stresses τ_i^* , according to authors AZT-M [25,28] and ESS [27] and others [17,26]. This conclusion, stemming from the theoretical solution, complies with the results of large-scale field tests conducted by V.A. Ilyichev, V.I. Kerchman, B.I. Rubin, and V.M. Pyatetsky [7,13] focused on the influence of static and dynamic loading.

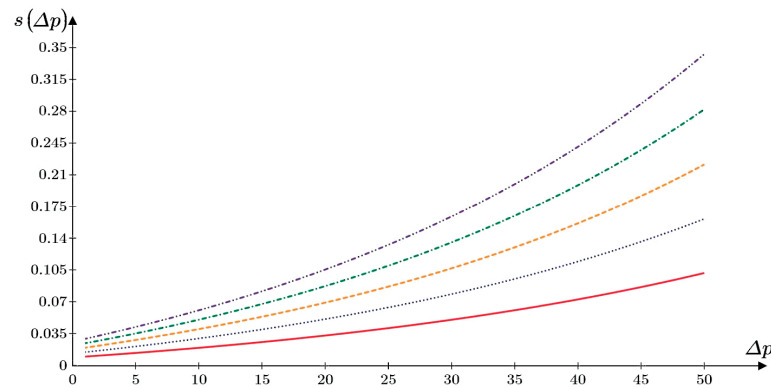


Figure 14. Dependence of the value of excessive foundation settlement on the value of the dynamic component of loading Δp at different values of the static component of loading p_1 : (—) $p_1 = 80$ kPa; (.....) $p_1 = 120$ kPa; (---) $p_1 = 160$ kPa; (-.-.-) $p_1 = 200$ kPa; (-.-.-.-) $p_1 = 240$ kPa.

If we take the values of the amplitude of vibrations and patterns of their propagation in plan and at depth from Formulas (6), (10), and (11), and analyze the propagation of viscoplastic settlement taking vibrocreep into account under dynamic loading according to Formula (3), we obtain the graph of settlement for a nearby foundation shown in Figure 15.

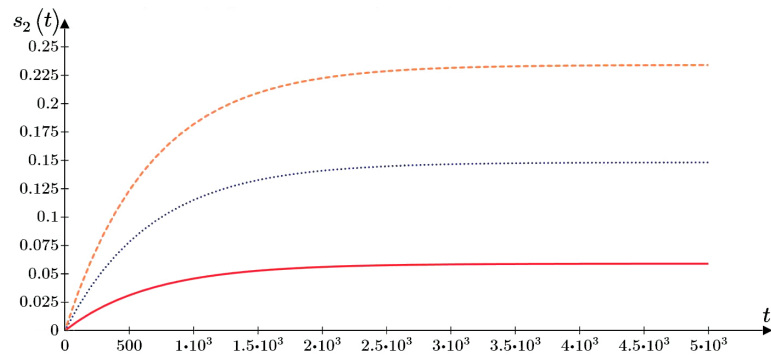


Figure 15. Foundation settlement propagation in time, if the value of static load $p_1 = 160$ kPa and dynamic load $\Delta p = 30$ kPa, triggered by the source foundation, when static load p_2 from the foundation of a nearby building is: (—) $p_2 = 160$ kPa; (.....) $p_2 = 240$ kPa; (---) $p_2 = 320$ kPa.

If the dynamic component $\Delta p = 30$ kPa and values of load p_2 are variable, the dependence of the value of excessive settlement of the foundation of a nearby building s_2 on the static load from the source foundation p_1 is as shown in Figure 16.

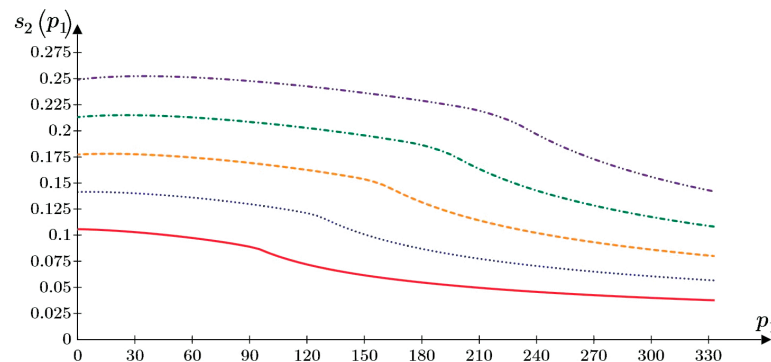


Figure 16. Dependence of the value of excessive settlement of the foundation of a nearby building s_2 on the static load from the source foundation p_1 if the dynamic component $\Delta p = 30$ kPa, the distance between foundations $c = 4.0$ m, and the load values p_2 : (—) $p_2 = 160$ kPa; (.....) $p_2 = 200$ kPa; (---) $p_2 = 240$ kPa; (-.-.-) $p_2 = 280$ kPa; (-.-.-.-) $p_2 = 320$ kPa.

4. Discussion

When analyzing the $s_2(p_1)$ graph (Figure 16), one can observe a decrease in the settlement of a nearby foundation with an increase in the static load from the source foundation p_1 , which can be explained by an increase in the difference between the intensity of shear stresses τ_i (Figure 17b) and their limiting value τ_i^* , which in turn depends on the value of mean stress σ_m (Figure 17a).

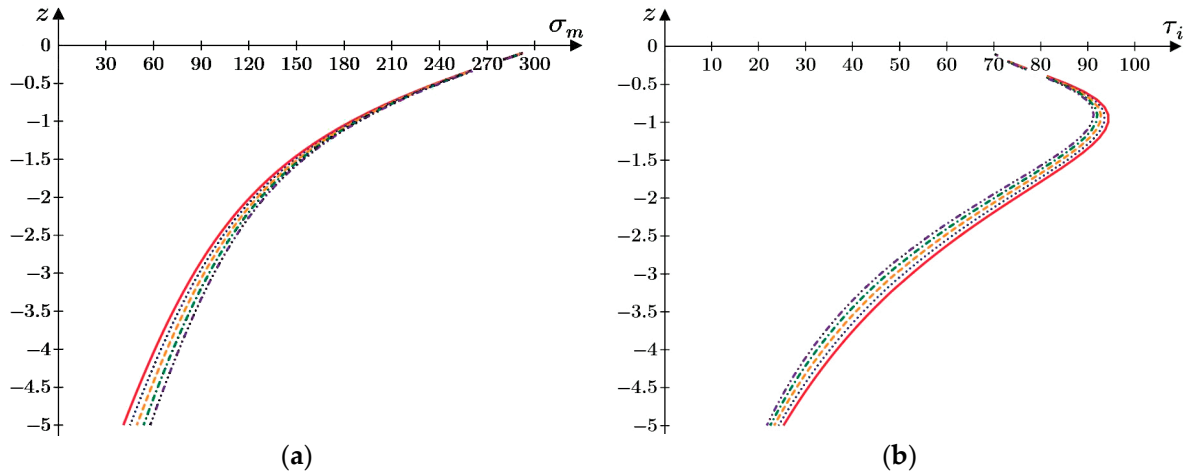


Figure 17. Dependence of stresses $\sigma_m(z)$ (a) and $\tau_i(z)$ (b) arising below the nearby foundation if loading $p_2 = 300$ kPa and loading values p_1 : (—) $p_1 = 160$ kPa; (.....) $p_1 = 200$ kPa; (---) $p_1 = 240$ kPa; (-.-.-) $p_1 = 280$ kPa; (-.-.-.-) $p_1 = 320$ kPa.

It will be more obvious to show the effect of the load from the source foundation p_1 on the settlement of the nearby foundation using the coefficient k_{ult} (12). This coefficient is part of Formula (3) and shows a decrease in the viscosity coefficient η_0 with the approach of the intensity of shear stresses τ_i to their limiting value τ_i^* . Figure 18 clearly shows an increase in the coefficient k_{ult} under the nearby foundation with an increase in the pressure p_1 of the source foundation.

$$k_{ult} = \frac{\tau_i^* - \tau_i}{\tau_i^*} \tag{12}$$

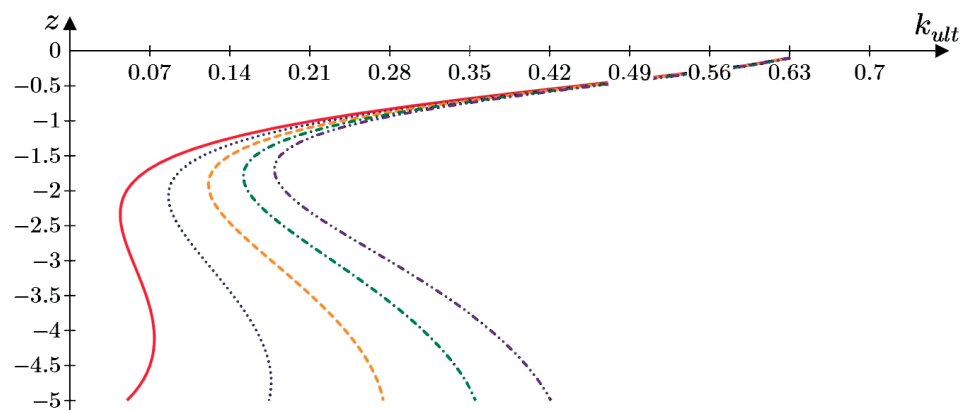


Figure 18. Dependence of the coefficient $k_{ult}(z)$ below the nearby foundation if loading $p_2 = 300$ kPa and loading values p_1 : (—) $p_2 = 160$ kPa; (.....) $p_2 = 200$ kPa; (---) $p_2 = 240$ kPa; (-.-.-) $p_2 = 280$ kPa; (-.-.-.-) $p_2 = 320$ kPa.

The static load from source foundation p_1 and the soil above the foundation base serve as the lateral surcharge concerning the nearby foundation. This lateral surcharge increases

mean stresses σ_m and reduces the intensity of shear stresses τ_i , thereby bringing the stress state a little closer to compression.

The above statement that the settlement of the nearby foundation s_2 decreases with increasing static pressure p_1 from the source foundation has some exceptions. As it can be seen, for large values of p_1 and small values of p_2 and c , the settlement of the nearby foundation s_2 increases with the growth of p_1 , and does not decrease. The graph in Figure 19 shows the peculiar shape of the two characteristic areas (approximately $p_1 < 150$ kPa and $p_1 > 150$ kPa), which require explanation. The first area (approximately $p_1 < 150$ kPa) shows an intensive decrease in the s_2 settlement caused by the loading of the zone of the soil uplift from under the base of the adjacent foundation. In this case, the size of the zone of plastic deformation propagation increases because the intensity of tangential stresses τ_i decreases and, thus, gets further from their limiting value τ_i^* (Figure 17b). Since the ratio of stresses τ_i and τ_i^* has a non-linear character, in the area of $p_1 \approx 150$ kPa the effect of an increase in lateral loading decreases, and the curve changes its direction. At the same time, if the distance between the foundations c is small and the load from nearby foundation p_2 is low, one can observe an increase in settlement s_2 in the case of considerable load from the source foundation p_1 (Figure 19, approximately $p_1 > 150$ kPa), which is explained by an increase in the intensity of shear stresses τ_i and small mean stress σ_m .

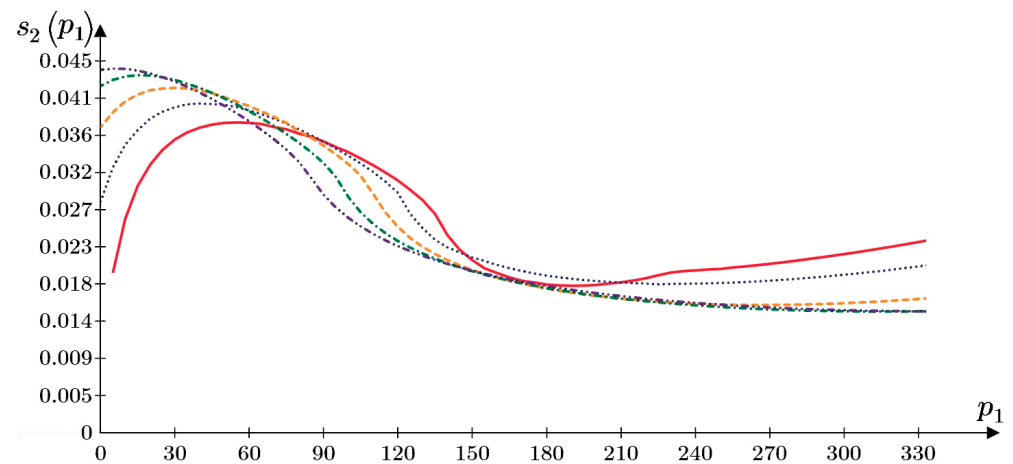


Figure 19. Dependence of the value of excessive settlement of the foundation of a nearby building s_2 on static load from the source foundation p_1 , if load $p_2 = 90$ kPa, dynamic component $\Delta p = 30$ kPa, and the distance between the foundations c : (—) $c = 0.0$ m; (.....) $c = 0.5$ m; (---) $c = 1.0$ m; (-.-.-) $c = 1.5$ m; (-.-.-.-) $c = 2.0$ m.

The graph, showing the dependence of the value of excessive settlement of a nearby foundation s_2 on the static load from source foundation p_2 , if the dynamic component $\Delta p = 30$ kPa and values of load p_1 are variable, is shown in Figure 20. Dependence of the effect of load from the source foundation p_1 on the value of excessive settlement of a nearby foundation s_2 can also be seen in Figure 16, where smaller values of load p_1 correspond to a larger value of settlement s_2 .

If the static load from the source foundation $p_1 = 160$ kPa, the dynamic component is $\Delta p = 30$ kPa, the load $p_2 = 350$ kPa, and the values of depth h_1 vary, the dependence of the value of excessive foundation settlement s_2 on the distance between the foundations c is as shown in Figure 21. The settlement of the nearby foundation s_2 nonlinearly decreases with an increase in the distance from the source foundation, which naturally follows from theoretical assumptions. At a distance of $c > 2b$, the effect of the transmitting foundation decreases significantly, and this fact converges with the numerical solution of Vivek P. and Ghosh P. [42] to the problem of the effect of a transmitting foundation that transmits static and dynamic loads to the base (an active foundation) on the additional settlement of an adjacent foundation that only transmits static loads to the base (a passive foundation).

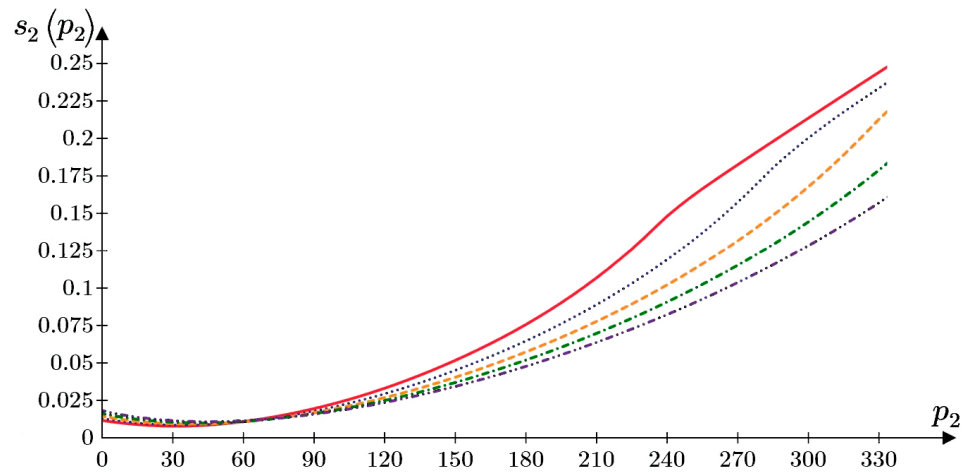


Figure 20. Dependence of the value of excessive settlement of a nearby building s_2 on static load from the source foundation p_2 with dynamic component $\Delta p = 30$ kPa and load p_1 : (—) $p_1 = 160$ kPa; (.....) $p_1 = 200$ kPa; (---) $p_1 = 240$ kPa; (-.-.-) $p_1 = 280$ kPa; (-.-.-.-) $p_1 = 320$ kPa.

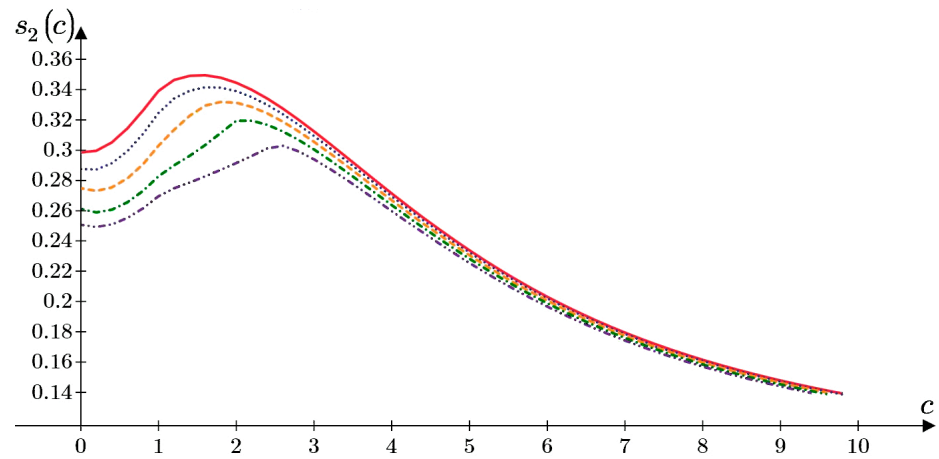


Figure 21. Dependence of excessive settlement of the foundation s_2 of a nearby building on the distance between foundations c , if the static load from the source foundation $p_1 = 160$ kPa, the dynamic component is $\Delta p = 30$ kPa, the load $p_2 = 350$ kPa, and the depth h_1 : (—) $h_1 = 1.0$ m; (.....) $h_1 = 2.0$ m; (---) $h_1 = 3.0$ m; (-.-.-) $h_1 = 4.0$ m; (-.-.-.-) $h_1 = 5.0$ m.

Settlement s_2 of the foundation located near the foundation that serves as the source of the dynamic effect (the source foundation) naturally increases with an increase in static pressure p_2 below its base (Figures 15 and 20); however, it decreases as the static component of the load from the source foundation p_1 and the depth of the foundation increase (Figures 16 and 19), which is explained by an increase in the difference between shear stress intensity τ_i and the limiting value τ_i^* , the first of which decreases as the stress state of the base approaches its limit value and the second of which increases due to the increasing mean stress σ_m (Figure 17). The theoretical solution to the problem, obtained by the current authors, complies with the results of the field studies conducted by V.S. Bogolyubchik, V.Y. Khain, and M.N. Goldstein [14–16] in respect of the effect of soil loading beyond the foundation on the vibrocreep intensity of a sandy base subjected to vibrations. It is quite natural that the excessive settlement of a nearby foundation decreases with increasing distance from the source foundation c and depth of the foundation h_1 (Figure 21), which is explained by a decrease in the value of vibratory acceleration and an increase in the viscosity coefficient [5,6,25–28]. The problem is solved for the value of the loading frequency $\omega = 10$ Hz. With a change in vibration frequency, the qualitative

pattern of vibration will remain the same, but the settlement will take greater values, as was identified earlier [27,28,50].

The above-mentioned conclusions were obtained for the case of flexible load transfer to the base without taking into account the stiffness of the foundations themselves and the superstructures of the construction. In the future, the solution to this problem can be developed by including the stiffness of building structures in the structural analysis, which should lead to a decrease in additional settlement.

The authors believe that this research can be furthered by developing a generalized rheological model of sandy soil subjected to cyclic loading. In his earlier work, one of the authors (AZT-M) remarked that lateral pressure increases under dynamic loading [25], which indicates a change in Poisson's ratio. In addition, AZT-M found that the phenomenon of vibrocreep is more pronounced when shear deformation prevails [25]. Further, the authors believe that more research is needed to study the effect of the dynamic load intensity on Poisson's ratio. They also intend to create a quantitative description of the effect of the stress–strain state of sandy soil on the intensity of vibrocreep, taking into account the Nadai-Lode parameter [54], as was done by K. Wang et al. [33]. The above-listed further research undertakings will generate important practical results that will allow for a more accurate projection of displacement of the soil massif and pressure on substructures subjected to dynamic loading.

5. Conclusions

Applying the analytical solution proposed by the authors, it was found that the settlement of a single foundation to which vertical static and dynamic loads are transmitted increases with an increase in its static and dynamic components. The dynamic component, which is triggered by viscoplastic shear of the double-sided extrusion type, makes a greater contribution to settlement propagation. The increase in settlement accompanying an increase in the dynamic component is due to a decrease in the viscosity coefficient that accompanies an increase in the vibratory acceleration of the base, while the increase in settlement that accompanies an increase in the static component is caused by an increase in the intensity of shear stresses in the base and those stresses approaching their limiting values.

The settlement of a foundation located in proximity to the foundation that is the source of dynamic effects naturally increases with an increase in static pressure below its base but decreases with an increase in the static component of the load from the source foundation and greater foundation depth, which is explained by an increase in the difference between the values of shear stresses intensity and their limiting values, the first of which decreases as the stress state of the foundation gets closer to compression, and the second of which increases due to an increase in the mean stress.

Author Contributions: Conceptualization, methodology, software, formal analysis, investigation, resources, data curation, A.Z.T.-M.; writing—original draft preparation, A.Z.T.-M., A.N.S. and E.S.S.; writing—review and editing, A.Z.T.-M.; visualization, A.Z.T.-M., A.N.S. and E.S.S.; supervision, project administration, funding acquisition, A.Z.T.-M. All authors have read and agreed to the published version of the manuscript.

Funding: This research was supported by the Ministry of Science and Higher Education of the Russian Federation (project No. FSWG-2023-0004, «A system of territorial seismic protection of critical infrastructure facilities based on granular metamaterials with the properties of wide-range phonon crystals»).

Data Availability Statement: The data used to support the findings of this study are included within the article. The original details of the data presented in this study are available on request from the corresponding author.

Conflicts of Interest: The authors declare no conflict of interest.

References

1. Ter-Martirosyan, A.Z.; Sobolev, E.S. Safe performance of bases of buildings and structures under dynamic impacts. *Vestn. MGSU* **2017**, *12*, 537–544. [\[CrossRef\]](#)
2. Chernov, Y.T. Design of buildings and structures exposed to dynamic influences. *Ind. Civ. Eng.* **2018**, *4*, 73–77.
3. Savinov, O.A. *Modern Designs of Foundations for Machines and Their Analysis*; Leningrad, Stroyizdat: Moscow, Russia, 1979; 200p.
4. Ma, L. Study on abnormal vibration caused by foundation settlement of a 650MW unit. *J. Phys. Conf. Ser.* **2021**, *1748*, 062032. [\[CrossRef\]](#)
5. Barkan, D.D. *Dynamics of Foundations*; McGraw-Hill Book Co.: New York, NY, USA, 1948; 411p.
6. Barkan, D.D. *Dynamics of Bases and Foundations*; McGraw-Hill Book Co.: New York, NY, USA, 1962; 434p.
7. Pyatetsky, V.M.; Alexandrov, B.K.; Savinov, O.A. *Modern Computer Designed Foundations and Their Automated Design*; Stroyizdat: Moscow, Russia, 1993; 415p.
8. Ivanov, P.L. *Soils and Bases of Hydraulic Structures. Mechanics of Soils: Textbook for Hydraulic Engineering Specialties of Universities*; Higher School: Moscow, Russia, 1991; 447p.
9. Krasnikov, N.D. *Dynamic Properties of Soils and Methods of Their Determination*; Leningrad, Stroyizdat: Moscow, Russia, 1970; 240p.
10. Ilyichev, V.A.; Mangushev, R.A. (Eds.) *Handbook of Geotechnics. Foundations, Foundations, and Underground Structures*; ASV Publishing House: Moscow, Russia, 2016; 1040p.
11. Shebunyaev, A.N. Review of the results of studies on the effect of vibrations on physical and mechanical properties of sandy soils. *Eng. Constr. Bull. Casp. Sea* **2022**, *3*, 15–22. [\[CrossRef\]](#)
12. Voznesensky, E.A. *Dynamic Instability of Soils*, 2nd ed.; Leningrad, Stroyizdat: Moscow, Russia, 2014; 264p.
13. Ilyichev, V.A.; Kerchman, V.I.; Rubin, B.I.; Piatetsky, V.M. Experimental study of sand soil vibrocreeping. In Proceedings of the International Symposium on Soil under Cyclic and Transient Loading, Swansea, UK, 7–11 January 1980; Volume 1, pp. 239–245.
14. Bogolyubchik, V.S.; Goldstein, M.N.; Khain, V.Y. Experimental field studies of vibrocreep of sandy and sandy loam foundations. Dynamics of foundations, foundations, and underground structures. In Proceedings of the 4th All-Union Conference, Tashkent, Uzbekistan, 16–18 November 1977; pp. 192–195.
15. Bogolyubchik, V.S.; Khain, V.Y. Flute Tests of Sand to Study Vibrocreep. In *The Collection "Voprosy Geotekhniki" № 22*; Dnepropetrovsk Institute of Railway Transport Engineers Named after L.M. Kaganovich: Dnepropetrovsk, Ukraine, 1973.
16. Hain, V.Y. *Study of the Time Dependence of Vibrocreep of a Sand Foundation Model. NTL, Subpart, B., Issue 6, № 215*; Moscow, Russia, 1975.
17. Gil, D.F.; Mendoza, C.C.; Vásquez-Varela, L.R.; Cano, S. Physical Model of Shallow Foundation under Dynamic Loads on Sands. *Infrastructures* **2022**, *7*, 147. [\[CrossRef\]](#)
18. Al-kaream, K.; Fattah, M.; Khaled, Z. Effect of the mode of vibration on the response of machine foundation on sand. In Proceedings of the IOP Conference Series: Materials Science and Engineering, 4th International Conference on Buildings, Construction and Environmental Engineering, Istanbul, Turkey, 7–9 October 2019; Volume 737. [\[CrossRef\]](#)
19. Wang, J.; Qi, H.; Lin, Z.; Tang, Y. Analysis of Dynamic Deformation Response of Closely Spaced Square Footings on Geogrid-Reinforced Sand under Cyclic Loading. *Sustainability* **2023**, *15*, 438. [\[CrossRef\]](#)
20. Casagrande, A.; Shannon, W.L. Research on stress deformation and strength characteristics of soils and soft rocks under transient loading. *Harv. Soil Mech. Ser.* **1948**, *31*.
21. Seed, H.B.; Lee, K.L. Liquefaction of saturated sands during cyclic loading. *J. Soil Mech. Found. Div. ASCE* **1966**, *92*, 105–134. [\[CrossRef\]](#)
22. Lee, K.L.; Focht, J. Liquefaction potential at the Ekofisk tank in the North Sea. *J. Geotech. Eng. Div. ASCE* **1975**, *101*, 1–18. [\[CrossRef\]](#)
23. Chaney, R.C.; Fang, H.Y. Response of non-saturated soil to cyclic loading. In Proceedings of the International Conference on Recent Advances in Geotechnical Earthquake Engineering and Soil Dynamics, St. Louis, MO, USA, 26 April–3 May 1981; Volume 2, p. 643.
24. Khosla, V.K.; Singh, R.D. Influence of number of cycles on strain. *Can. Geotech. J.* **1978**, *15*, 584–592. [\[CrossRef\]](#)
25. Ter-Martirosyan, A.Z. *Interaction of Foundations with the Base under Cyclic and Vibration Influences Taking into Account Rheological Properties of Soils*; NRU MGSU: Moscow, Russia, 2010; 190p.
26. Ter-Martirosyan, A.Z.; Sobolev, E.S. Long-term vibration laboratory tests of sandy soils. *IOP Conf. Ser. Mater. Sci. Eng.* **2021**, *1015*, 012051. [\[CrossRef\]](#)
27. Sobolev, E.S. *Creep and Vibrocreep of Sandy Soils of Foundations of Buildings and Structures*; NRU MGSU: Moscow, Russia, 2014; 150p.
28. Ter-Martirosyan, A.Z. *Interaction of Foundations of Buildings and Structures with Saturated Foundations Taking into Account Nonlinear and Rheological Properties of Soils*; NRU MGSU: Moscow, Russia, 2016; 324p.
29. Ter-Martirosyan, Z.; Sobolev, E.; Ter-Martirosyan, A. Rheological Properties of Sandy Soils. *Adv. Mater. Res.* **2014**, *1073–1076*, 1673–1679. [\[CrossRef\]](#)
30. Liu, X.; Li, S.; Lin, L.; Li, T.; Yin, J. Experimental Study on the Monotonic and Cyclic Behaviour of Carbonate Sand in the South China Sea. *KSCE J. Civ. Eng.* **2021**, *25*, 3254–3263. [\[CrossRef\]](#)
31. Poblete, M.; Wichtmann, T.; Niemunis, A.; Triantafyllidis, T. Accumulation of residual deformations due to cyclic loading with multidimensional strain loops. In Proceedings of the Fifth International Conference on Earthquake Geotechnical Engineering, Santiago, Chile, 9–14 January 2011.

32. Kafle, B.; Wuttke, F. Response of Shallow Foundation Under Coupled Cyclic Loading For Unsaturated Sand at Large Number of Cycles. *Jpn. Geotech. Soc. Spec. Publ.* **2019**, *7*, 525–530. [[CrossRef](#)]
33. Wang, K.; Chen, Z.; Wang, Z.; Chen, Q.; Ma, D. Critical Dynamic Stress and Cumulative Plastic Deformation of Calcareous Sand Filler Based on Shakedown Theory. *J. Mar. Sci. Eng.* **2023**, *11*, 195. [[CrossRef](#)]
34. Jianhong, Y.; Haiyilati, Y.; Cao, M.; Zuo, D.; Chai, X. Creep characteristics of calcareous coral sand in the South China Sea. *Acta Geotech.* **2022**, *17*, 5133–5155. [[CrossRef](#)]
35. Dong-Ning, D.; Lai-Gui, W.; Zhang, X.; Shu-Kun, Z. Study on sand particles creep model and open pit mine landslide mechanism caused by sand fatigue liquefaction. In Proceedings of the IOP Conference Series: Earth and Environmental Science, 3rd International Conference on Advances in Energy, Environment and Chemical Engineering, Chengdu, China, 26–28 May 2017; Volume 69. [[CrossRef](#)]
36. Liu, Y.; Liang, Z.; Liu, Z.; Nie, G. Post-Cyclic Drained Shear Behaviour of Fujian Sand under Various Loading Conditions. *J. Mar. Sci. Eng.* **2022**, *10*, 1499. [[CrossRef](#)]
37. Wang, Z.; Zhang, L. Experimental Study on Dynamic Parameters of Calcareous Sand Subgrade under Long-Term Cyclic Loading. *J. Mar. Sci. Eng.* **2022**, *10*, 1806. [[CrossRef](#)]
38. Kumar, A.; Azizi, A.; Toll, D. The Influence of Cyclic Loading Frequency on the Response of an Unsaturated Railway Formation Soil. *Geo-Congr.* **2022**, *2022*, 274–283. [[CrossRef](#)]
39. Song, D.; Liu, H.; Sun, Q. Significance of Determination Methods on Shear Modulus Measurements of Fujian Sand in Cyclic Triaxial Testing. *Appl. Sci.* **2022**, *12*, 8690. [[CrossRef](#)]
40. Ma, W.; Qin, Y.; Gao, F.; Wu, Q. Experimental Study of the Dynamic Shear Modulus of Saturated Coral Sand under Complex Consolidation Conditions. *J. Mar. Sci. Eng.* **2023**, *11*, 214. [[CrossRef](#)]
41. Xia, P.; Shao, L.; Deng, W.; Zeng, C. Evolution Prediction of Hysteresis Behaviour of Sand under Cyclic Loading. *Processes* **2022**, *10*, 879. [[CrossRef](#)]
42. Vivek, P.; Ghosh, P. Dynamic interaction of two nearby machine foundations on homogeneous soil. In Proceedings of the GeoCongress 2012. State of the Art and Practice in Geotechnical Engineering, Oakland, CA, USA, 25–29 March 2012; pp. 21–30.
43. Wichtmann, T.; Niemunis, A.; Triantafyllidis, T. Differential settlements due to cyclic loading and their effect on the lifetime of structures. In Proceedings of the 3rd International Conference on Lifetime Oriented Design Concepts, Freiburg, Germany, 12–14 November 2007.
44. Wuttke, F.; Schmidt, H.G.; Zabel, V.; Kafle, B.; Stade, I. Vibration Induced Building Settlement Assessment and Calculation. In Proceedings of the 8th International Conference on Structural Dynamics EURODYN, Leuven, Belgium, 4–6 July 2011.
45. Yi, F. Procedure to evaluate seismic settlement in dry sand based on shear wave velocity. In Proceedings of the 9th U.S. National and 10th Canadian Conference on Earthquake Engineering (9USN/10CCEE), Toronto, ON, Canada, 25–29 July 2010. [[CrossRef](#)]
46. Yi, F. Procedures to evaluate seismic settlement of dry sand based on CPT data, an update. In Proceedings of the 5th International Symposium on Cone Penetration Testing, Bologna, Italy, 8–10 June 2022; ISBN 9781003308829.
47. Pradel, D. Procedure to Evaluate Earthquake-Induced Settlements in Dry Sandy Soils. *J. Geotech. Geoenviron. Eng.* **1998**, *124*, 364–368. [[CrossRef](#)]
48. Sobolev, E.; Morev, D. The industrial buildings settlement foundations calculation made taking into account the soils vibro-creep. *IOP Conf. Ser. Mater. Sci. Eng.* **2019**, *698*, 022038. [[CrossRef](#)]
49. Geniev, G.A.; Estrin, M.I. *Dynamics of Plastic and Loose Medium. TsNIISK im. V.A. Kucherenko*; Stroyizdat: Moscow, Russia, 1972; 216p.
50. Ter-Martirosyan, Z.G.; Ter-Martirosyan, A.Z.; Sobolev, E.S. Creep and vibrocreep of sandy soils. *J. Eng. Res.* **2014**, *5–6*, 24–28.
51. Zhang, B.; Chen, K.; Hu, X.; Zhang, X.; Luo, G. Deformation constitutive model of subgrade soil under intermittent cyclic loading. *Sci. Rep. Nat. Publ. Group* **2023**, *13*, 301. [[CrossRef](#)]
52. Ukhov, S.B.; Semenov, V.V.; Znamensky, V.V.; Ter-Martirosyan, Z.G.; Chernyshev, S.N. *Mechanics of Soils, Bases, and Foundations—Textbook*; ASV Publishing House: Moscow, Russia, 2005; 528p.
53. Mei, C. *Mathematical Analysis in Engineering: How to Use the Basic Tools*; Cambridge University Press: Cambridge, UK, 1995.
54. Ter-Martirosyan, Z.G.; Ter-Martirosyan, A.Z. *Mechanics of Soils in High-Rise Construction with Exploitable Underground Parts—Textbook*; ASV Publishing House: Moscow, Russia, 2020; 946p.
55. Dacorogna, B.; Tanteri, C. *Mathematical Analysis for Engineers*; Imperial College Press: London, UK, 2012.
56. Maxfield, B. *Engineering with Mathcad: Using Mathcad to Create and Organize Your Engineering Calculations*; Butterworth-Heinemann: London, UK, 2006.
57. Vick, B. *Applied Engineering Mathematics*; CRC Press: Boca Raton, FL, USA, 2020.
58. Kerchman, V.I. Taking account of vibrocreep of sandy soils when designing foundations, accepting dynamic impacts. Dynamics of foundations, foundations, and underground structures. In Proceedings of the 4th All-Union Conference, Tashkent, Uzbekistan, 16–18 November 1977; pp. 205–207.

Disclaimer/Publisher’s Note: The statements, opinions and data contained in all publications are solely those of the individual author(s) and contributor(s) and not of MDPI and/or the editor(s). MDPI and/or the editor(s) disclaim responsibility for any injury to people or property resulting from any ideas, methods, instructions or products referred to in the content.